*IN-17*

*207545*

*14 P*

NASA Technical Memorandum 106484

# Bounds and Simulation Results of 32-ary and 64-ary Quadrature Amplitude Modulation for Broadband-ISDN via Satellite

Muli Kifle
*National Aeronautics and Space Administration*
*Lewis Research Center*
*Cleveland, Ohio*

and

Mark Vanderaar
*Sverdrup Technology, Inc.*
*Lewis Research Center Group*
*Brook Park, Ohio*

February 1994

**NASA**

# Bounds and Simulation Results of 32-ary and 64-ary Quadrature Amplitude Modulation for Broadband-ISDN via Satellite

Muli Kifle
NASA Lewis Research Center
21000 Brookpark Rd.
Cleveland, Ohio 44135

Mark Vanderaar*
Sverdrup Technology, Inc.
2001 Aerospace Parkway
Brook Park, Ohio 44142

*Abstract* - Union bounds and Monte Carlo simulation Bit-Error-Rate (BER) performance results are presented for various *32-ary* and *64-ary* Quadrature Amplitude Modulation (QAM) schemes. Filtered and unfiltered modulation formats are compared for the best packing arrangement in peak power limited systems. It is verified that circular constellations which populate as many symbols as possible at the peak magnitude offer the best performance. For example a *32-ary* QAM scheme based on concentric circles offers about *1.05 dB* better peak power improvement at a BER of $10^{-6}$ over the scheme optimized for average power using triangular symbol packing. This peak power improvement increases to *1.25 dB* for comparable *64-ary* QAM schemes.

This work is serves as a precursor to determine the feasibility of a combined modem/codec that can accommodate Broadband Integrated Services Digital Network (B-ISDN) at a rate of *155.52 Mbps* through typical transponder bandwidths of *36 MHz* and *54 MHz*.

## I. INTRODUCTION

In order for B-ISDN to be successfully used across satellite links, techniques must be developed to accommodate the data rates using existing satellite transponders. Present and planned transponders and ground terminals commonly have either *36, 54, or 72 MHz* bandwidths [1]. The state-of-the-art in bandwidth and power efficient modems for B-ISDN achieves the *155.52 Mbps* through a *72 MHz* INTELSAT transponder [2]. Accommodating B-ISDN through the narrower *36* and *54 MHz* bandwidths requires a significant increase in bandwidth efficiency without incurring too severe of a power penalty. The theoretically minimum power required for error-free transmission of *155.52 Mbps* through linear *54* and *36 MHz* transponders is approximately *3.44 dB* $E_b/N_o$ and *6.43 dB* $E_b/N_o$, respectively. In practice, these limits are not achievable with reasonable hardware complexity. In terms of bandwidth, assuming *40%* raised cosine pulse-shaping, *32-ary* QAM could transmit *155.52 Mbps* in *43.55 MHz*. Thus, if overhead for error-corrective coding is accounted for, *32-ary* QAM is suitable for transmitting *155.52 Mbps* in *54 MHz* transponders. Under the same assumptions, *64-ary* QAM appears suitable for *36 MHz* transponders. The goal is to obtain practical schemes that have power performance on the same order as that of QPSK. It is expected that the increase in bandwidth efficiency will result in a power penalty that can be

absorbed through the use of advanced High Power Amplifiers (HPAs) such as hybrid solid state / TWT amplifiers or increased ground terminal antenna sizes.

Section II of this paper discusses some system issues concerning nonlinear signal amplification. Section III discusses the effect of shaping filters in the nonlinear environment. Section IV develops the modulation schemes used. Section V develops and evaluates analytical bounds on the performance of the modulation schemes. Time domain simulation results are presented and compared to the bounds in Section VI. Finally, conclusions are drawn from the results that point towards future work.

## II. HIGH POWER AMPLIFIER CHARACTERISTICS

The performance of High Power Amplifiers (HPAs) for satellite communications is bounded by both average prime (satellite DC) power and peak transmitted (RF) power. One overall system design goal for satellite HPAs is to obtain the highest data throughput for the minimum satellite prime power. For this reason, HPAs are designed for the maximum efficiency (the ratio of RF power out to DC power in) and linearity (AM to AM and AM to PM distortion measurements). However, as RF devices, HPAs will always have residual nonlinear characteristics, particularly near saturation. In the case of single channel per HPA systems, the nonlinearities can be significantly reduced through the use of predistortion and equalization techniques. References [3] - [7] address the details of predistortion and equalization in QAM systems.

For this study, it will be assumed that the overall transmit chain including the HPA can be modelled by an ideal clipping limiter. The amplitude response of an ideal clipping limiter can be described as

$$P_{out} = \begin{cases} G P_{in}, & P_{in} < P_{in\ sat} \\ P_{out\ sat}, & P_{in} \geq P_{in\ sat} \end{cases}$$

where $G$ is the power gain of the transmitter $P_{in}$ in the input power, $P_{out}$ is the output power, $P_{in\ sat}$ is the input power that saturates the amplitude response of the transmitter, and $P_{out\ sat}$ is the output power at input saturation and beyond.

Figure 1 illustrates that the gain is linear up to the saturated value of the HPA. A similar assumption can be

made for describing the amplitude to phase response as constant throughout the operating range, contributing no phase distortion to the system. The limiter response implies that peak power is an important design criteria for a modulation scheme. Further, due to the "linearized" nature of the overall channel, non-constant envelope schemes such as QAM are good choice for overall bandwidth and power efficiency. It should be noted that a real system, even after linearization and predistortion, will not have the theoretical ideal limited response due to hardware imperfections. This "implementation loss" is expected to be of greater concern for the higher order modulations studied here.
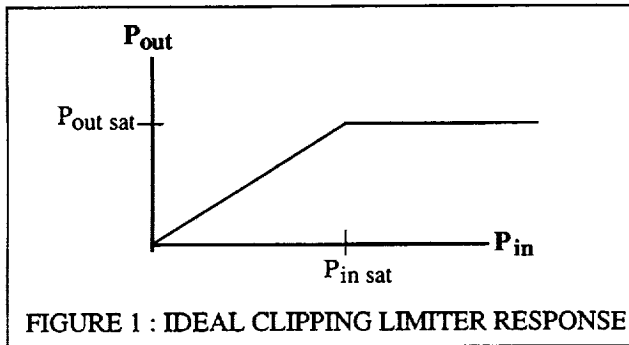


$P_{out}$

$P_{out\ sat}$

$P_{in}$

$P_{in\ sat}$

FIGURE 1 : IDEAL CLIPPING LIMITER RESPONSE

## III. BASEBAND FILTERING CONSIDERATIONS

In a practical communications system, the baseband modulated data is typically filtered at both the modulator and demodulator to meet allocated bandwidth requirements. These pulse shaping filters are designed to minimize bandwidth without introducing intersymbol interference (ISI). A common shaping filter is the square root raised cosine (SRRC) pulse shape. The frequency response of the SRRC is defined by

$$H(f) = \begin{cases} \dfrac{\pi T_s}{\pi(1-\beta)+4\beta}, & 0 \leq \left|\dfrac{f}{f_h}\right| \leq 1-\beta \\[2ex] \dfrac{\pi T_s}{\pi(1-\beta)+4\beta}\cos\left[\dfrac{\pi}{4\beta}\left(\left|\dfrac{f}{f_h}\right|-1+\beta\right)\right], & 1-\beta \leq \left|\dfrac{f}{f_h}\right| \leq 1+\beta \\[2ex] 0, & 1+\beta \leq \left|\dfrac{f}{f_h}\right| \end{cases}$$

where $T_s$ is the symbol period in seconds, $\beta$ is the rolloff rate, and $f_h$ is the half-amplitude frequency which equals $1/2T_s$. The impulse response of the SRRC is

$$h(t) = \left[\frac{4\beta}{\pi(1-\beta)+4\beta}\right]\left[\frac{T_s\,\alpha}{4\beta\,t} + \frac{\delta + \dfrac{4\beta\,t}{T_s^3}\alpha}{1 - \left(\dfrac{4\beta\,t}{T_s}\right)^2}\right]$$

where

$$\alpha = \sin\left[\frac{\pi\,(1-\beta)t}{T_s}\right] \quad \text{and} \quad \delta = \cos\left[\frac{\pi\,(1+\beta)t}{T_s}\right]$$

Further, $h(0) = 1$ and

$$h\left(\frac{\pm T_s}{4\beta}\right) = \left[\frac{4\beta}{\pi(1-\beta)+4\beta}\right]\left[\frac{\sin\left[\frac{\pi}{4\beta}(1-\beta)\right]}{2} + \frac{\pi\left(\cos\left[\frac{\pi}{4\beta}\right]+\sin\left[\frac{\pi}{4\beta}\right]\right)}{4\sqrt{2}}\right]$$

As mentioned, using the SRRC can significantly reduce the amount of bandwidth required to transmit the modulated signals. However, the SRRC filtered waveform is more sensitive than an unfiltered waveform to symbol timing offset and jitter.

Another important repercussion of filtering is that the peak power level is no longer associated with a constellation point but rather a signal trajectory associated with the filtered waveform. Figure 2 shows the effect of filtering a QPSK signal constellation with *40%* SRRC pulse shaping. Without filtering, the peak signal amplitude was the square root of two. The figure shows that a number of filtered trajectories exceed that level.
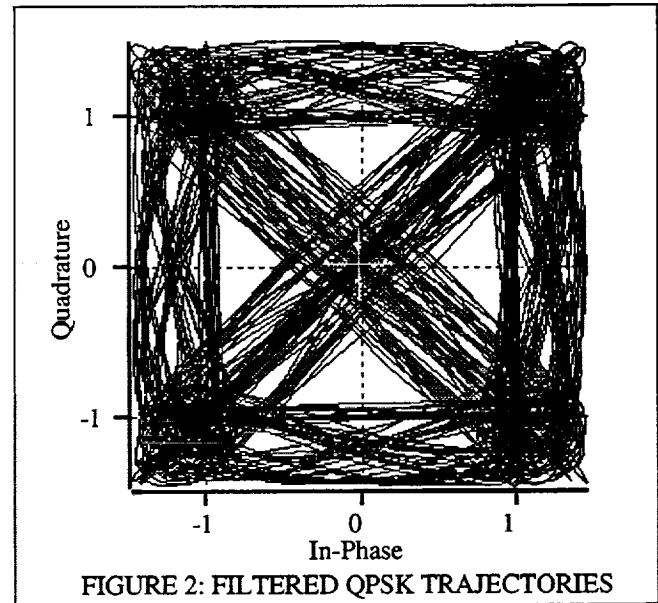


FIGURE 2: FILTERED QPSK TRAJECTORIES

Since the largest amplitude trajectory must be accommodated in the linear portion of the clipping channel, it defines the operating region of the modulation. It is therefore useful to determine the maximum of this trajectory in comparison to the peak constellation point in order to obtain a ratio that corresponds to a link margin loss due to filtering. The peak excursions of a signalling constellation occurs when a certain series of symbol pulse shapes add. This peak excursion value is found by adding samples of the SRRC

2

that are offset by one symbol time. This can be represented by

$$h_{sumj} = \sum_{i=1}^{a} h(j + is), \quad j = 1,2,3....,s$$

$$A_{peak} = \max \left( h_{sum} \right)$$

where $s$ is the number of samples per symbol and $a$ is the number of symbols considered, or aperture. The power of $A_{peak}$ needs to be compared to the peak power in the unfiltered two-dimensional modulation. If the unfiltered modulation waveform's power is normalized to the square root of 2, the peak filtered to unfiltered power ratio, $P_r$, is simply

$$P_r = \frac{\sqrt{A_{peak}^2 + A_{peak}^2}}{\sqrt{2}} = A_{peak}$$

Table 1 lists $P_r$ for a set of root raised cosine filtered signals with various rolloff factors. The SRRC was evaluated with an aperture that spanned 20 symbols. The table indicates that as the rolloff factors decrease, the peak signal power increases. For a rolloff factor of 0.1, the increase in peak power is 4.58 dB. For a more practical rolloff factor of 0.4 the increase in peak power is 3.62 dB. However, smaller rolloff factors result in less spectral occupancy. This decreased spectral occupancy in turn results in a reduction of the noise bandwidth that is manifested in an increase in $E_s/N_o$. The table also lists the $P_n$, the increase in $E_s/N_o$, as compared to a baseline "unfiltered" system that is defined to have a noise bandwidth that spans the main lobe of the signalling constellation. The last column in the table lists $P_{net}$, the net increase in required peak power, calculated as the increase in peak power minus the reduction in noise power. As the table shows, for all rolloff factors this is approximately 2 dB.

**TABLE 1**
EFFECT OF SRCC FILTERING ON PEAK POWER

| ß | Pr | Pr (dB) | Pn (dB) | Pnet (dB) |
|---|----|---------|---------|-----------|
| 0.1 | 2.87 | 4.58 | 2.60 | 1.98 |
| 0.2 | 2.63 | 4.20 | 2.22 | 1.99 |
| 0.3 | 2.45 | 3.88 | 1.87 | 2.01 |
| 0.4 | 2.30 | 3.62 | 1.55 | 2.07 |
| 0.5 | 2.16 | 3.34 | 1.25 | 2.09 |
| 0.6 | 2.02 | 3.06 | 0.97 | 2.09 |
| 0.7 | 1.90 | 2.79 | 0.71 | 2.08 |
| 0.8 | 1.83 | 2.63 | 0.46 | 2.17 |
| 0.9 | 1.79 | 2.53 | 0.22 | 2.31 |
| 1.0 | 1.69 | 2.27 | 0.00 | 2.27 |

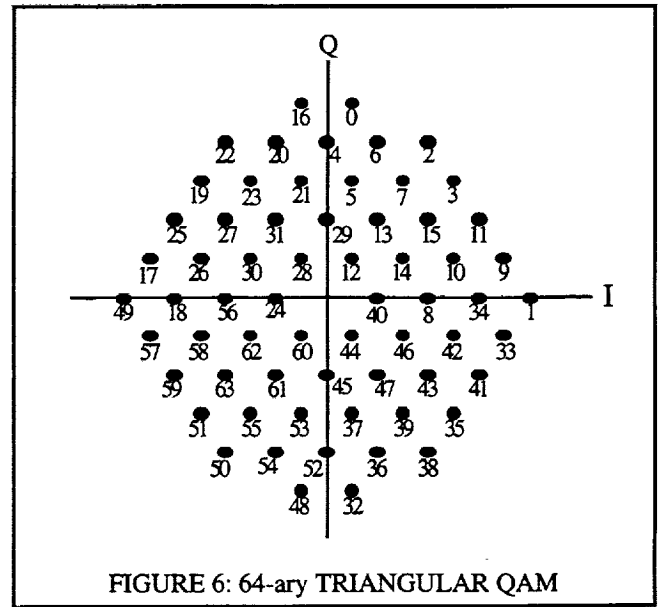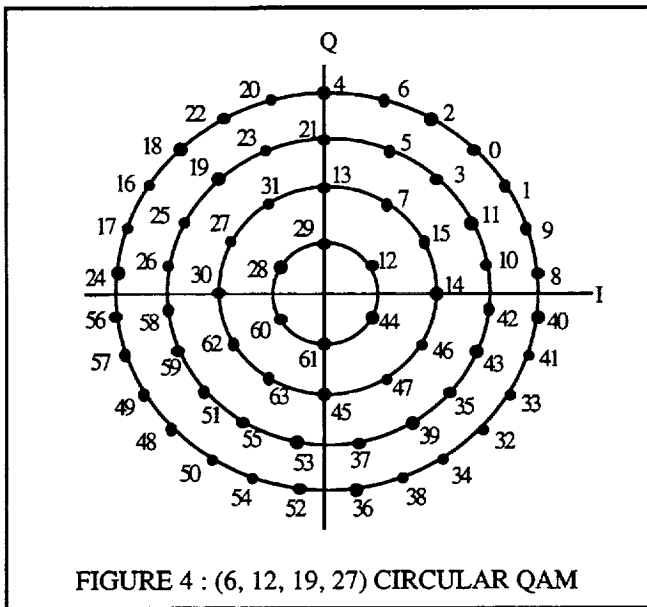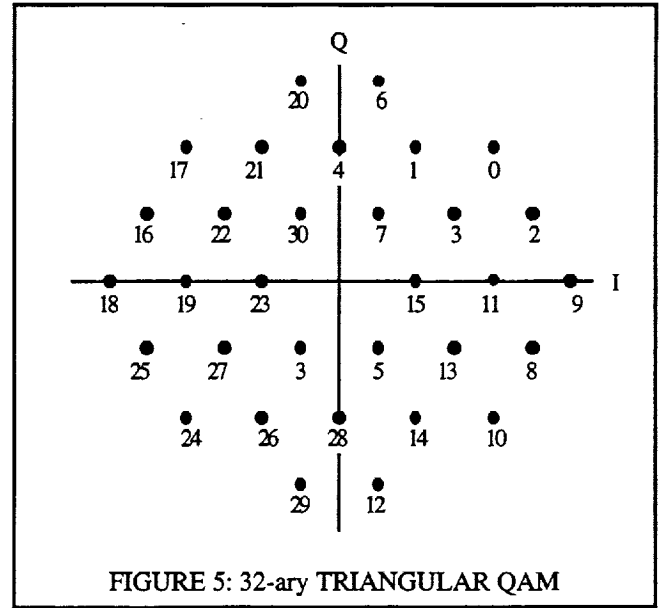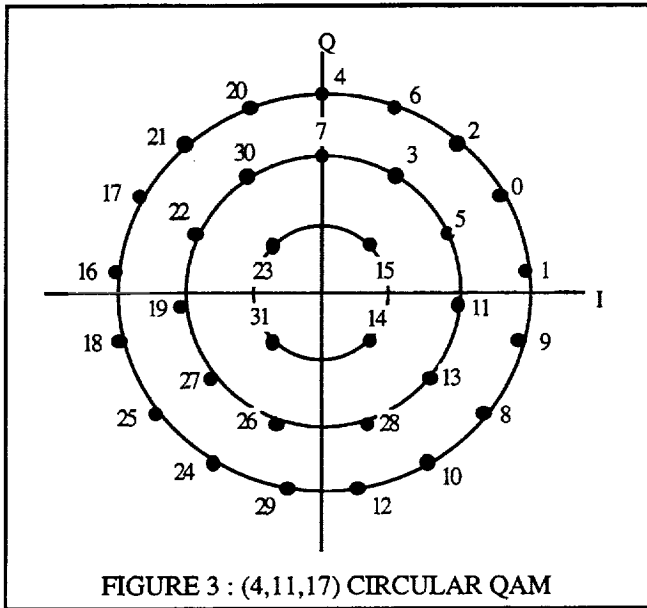There may be some techniques to limit the significant degradation caused by the peak trajectory power. For example, in an error corrective coded system, the symbol sequences may be constrained so as to prevent the highest excursions from occuring. Also, the effect caused by clipping the highest excursion on both the BER and bandwidth efficiency should be examined. In either case, the degradation may drop below 2 dB.

## IV. MODULATION FORMATS AND BIT-TO-SYMBOL MAPPINGS

Two types of 64-ary and 32-ary constellations are considered for evaluation. The first type has symbols arranged on concentric circles, the second has symbols arranged on a triangular grid, and the third type has symbols arranged on a rectangular grid [9]. In two-dimensions the arrangement on the triangular grid (called hexagonal packing) results in the best symbol error rate for average power limited systems. However, this is not necessarily the case in peak power limited systems. The 32-ary circular QAM design consists of three circles with four, eleven, and seventeen signals corresponding to the center circle, middle circle, and outside circle, respectively as shown in Figure 3. Similarly, for the 64-ary QAM signal sets , the circular design consists of four circles with six, twelve, nineteen, and twenty seven signals corresponding to the inner circle, second larger circle, third larger circle , and outside circle, respectively as shown Figure 4. The circular designs were chosen to approximate a uniform signal distribution as in [9]. A small improvement in performance may be gained by modifying the radii and rotations of the concentric circles. Further, Figures 5 - 8 show the mapping of the rectangular and triangular configurations of both 32-ary QAM and 64-ary QAM signal constellations.

Unfortunately, there is no known simple technique for optimally mapping constellation symbols to information bits other than in the case of a "square" constellation. In general, there are $M!$ possible mappings. When $M$ is large, it becomes computationally unreasonable to search for the best mapping. For instance: when $M=32$, there will be $32!=2.6313E+35$ possible constellation mappings.

A technique to heuristically find good signal mappings for rectangular, circular, and triangular constellations was used for this study. The performance of each mapping is evaluated by comparing the BER curves to bounds defined by the analytical expression of the symbol error probability as discussed in Section V. The technique is most easily described with the 64-ary rectangular QAM signal constellation. First, a 16-ary gray-coded rectangular QAM [7] is mapped on the upper right quadrant of the IQ with only one bit of a symbol differing from the corresponding bit of any nearest neighbors. A mirror image of the upper right quadrant across the Q-axis is taken to map another 16-ary gray-coded rectangular QAM on the upper left quadrant of the IQ plot. Similarly, a mirror image of both upper quadrants of the IQ plot across the I-axis is again taken to map on both bottom quadrants.

FIGURE 3 : (4,11,17) CIRCULAR QAM



FIGURE 5: 32-ary TRIANGULAR QAM



FIGURE 4 : (6, 12, 19, 27) CIRCULAR QAM



FIGURE 6: 64-ary TRIANGULAR QAM

By adding two extra bits, with four possible combinations and one of those four assigned per quadrant, on left side of each symbol , the optimum rectangular signal constellation for a *64-ary* QAM scheme is then successfully constructed. Even though similar techniques were applied in mapping the circular and triangular signal constellations, the constellations may not be optimum due to the nature of non-uniform distances between all nearest neighbors of a signal set. The mappings of all the constellations are shown in Tables 2 and 3.

The relative performance of this mapping technique is measured by comparing the closeness of the BER curves of any signal constellation to the "lower" bound or between the "lower" and random bounds that are developed in Section V. Figures 9 - 14 show simulation results obtained in all signal constellations. The results of the rectangular constellation for both *32-ary* QAM and *64-ary* QAM schemes verified the success of the mapping technique since the BER curves are near the bounds of the BER curve defined by the analytical expressions.
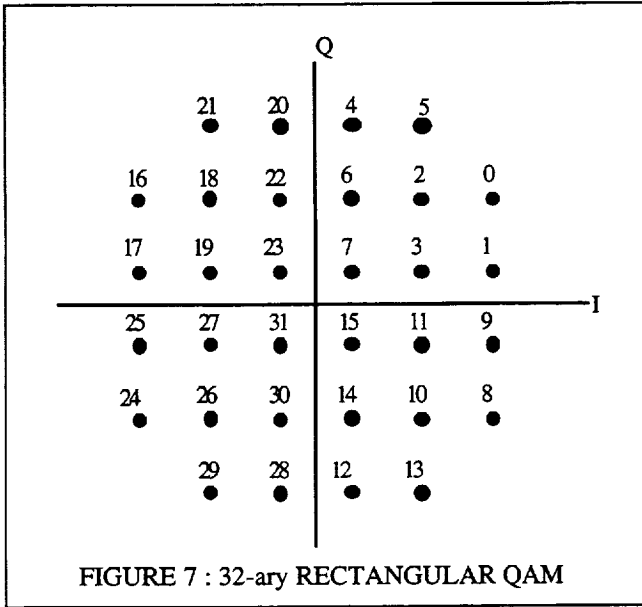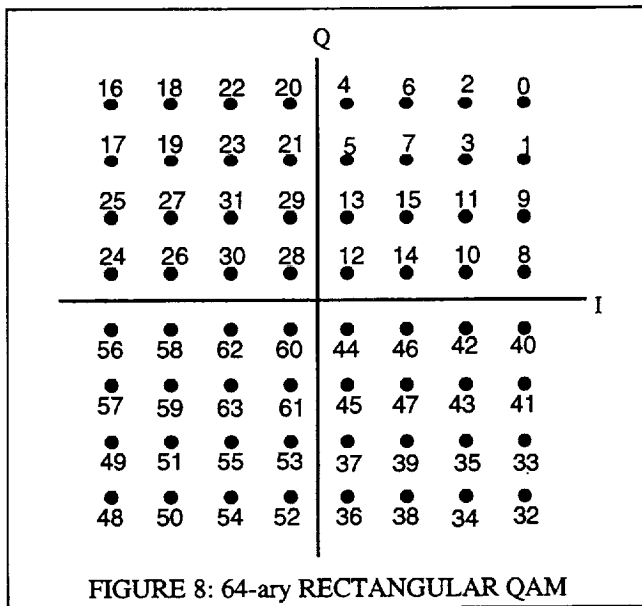
4

FIGURE 7 : 32-ary RECTANGULAR QAM



FIGURE 8: 64-ary RECTANGULAR QAM

## V. ANALYTICAL BOUNDS ON BIT-ERROR-RATE PERFORMANCE

The bit error probability of any M-ary modulation scheme in Additive White Gaussian Noise (AWGN) is dependent on both the Euclidean distance properties of the constellation and the Hamming distance of the bit to symbol mappings. Due to the complexity of the decision regions in a general M-ary QAM format, an exact analytical expression for the bit error rate is not easily evaluated. However, using a slight modification to the expression in [9], the upper bound on the symbol error

probability that is asymptotically tight at high signal to noise ratios is

$$P_s \leq \frac{2}{M}\sqrt{\frac{1}{2\pi}} \sum_{i=1}^{M-1} \sum_{j=i+1}^{M} \frac{\exp\left(-|S_i - S_j|^2 / 2\sigma^2\right)}{|S_i - S_j| / \sigma}$$

where the standard deviation is defined as

$$\sigma = \sqrt{\frac{1}{2E_s/N_0}}$$

and $S_i$ is the complex signal level of the $i'th$ of $M$ symbols in the constellation. It should be noted that $E_s/N_0$ can be evaluated based on peak or average signal energies. In this study, $E_s$ is defined as the peak energy of the modulation. As discussed in Section II adjustments can be made to compare peak signal energy in unfiltered or baseband filtered systems.

From the expression of the symbol error probability, bounds on the bit error probability can be determined. An upper bound is determined if each symbol error is assumed to result in the maximum number of bit errors. For an $M$-ary modulation format this can be written as

$$P_{b\ upper} = P_s$$

**TABLE 2**
**SYMBOL MAPPINGS FOR 32-ary QAM SCHEME**

| SYMBOL | BITS | CIRCULAR I | Q | RECTANGULAR I | Q | TRIANGULAR I | Q |
|---|---|---|---|---|---|---|---|
| 0 | 00000 | 2.399 | 1.195 | 5.0 | 3.0 | 4.0 | 3.464 |
| 1 | 00001 | 2.669 | 0.247 | 5.0 | 1.0 | 2.0 | 3.464 |
| 2 | 00010 | 1.806 | 1.981 | 3.0 | 3.0 | 5.0 | 1.732 |
| 3 | 00011 | 0.93 | 1.447 | 3.0 | 1.0 | 3.0 | 1.732 |
| 4 | 00100 | 0.00 | 2.68 | 1.0 | 5.0 | 0.0 | 3.464 |
| 5 | 00101 | 1.565 | 0.715 | 3.0 | 5.0 | 1.0 | -1.732 |
| 6 | 00110 | 0.968 | 2.499 | 1.0 | 3.0 | 1.0 | 5.196 |
| 7 | 00111 | 0.00 | 1.72 | 1.0 | 1.0 | 1.0 | 1.732 |
| 8 | 01000 | 2.139 | -1.615 | 5.0 | -3.0 | 5.0 | -1.732 |
| 9 | 01001 | 2.578 | -0.733 | 5.0 | -1.0 | 6.0 | 0.00 |
| 10 | 01010 | 1.411 | -2.279 | 3.0 | -3.0 | 4.0 | -3.464 |
| 11 | 01011 | 1.702 | -0.245 | 3.0 | -1.0 | 4.0 | 0.00 |
| 12 | 01100 | 0.492 | -2.634 | 1.0 | -5.0 | 1.0 | -5.196 |
| 13 | 01101 | 1.30 | -1.126 | 3.0 | -5.0 | 3.0 | -1.732 |
| 14 | 01110 | 0.50 | -0.50 | 1.0 | -3.0 | 2.0 | -3.464 |
| 15 | 01111 | 0.50 | 0.50 | 1.0 | -1.0 | 2.0 | 0.00 |
| 16 | 10000 | -2.669 | 0.247 | -5.0 | 3.0 | -5.0 | 1.732 |
| 17 | 10001 | -2.399 | 1.195 | -5.0 | 1.0 | -4.0 | 3.464 |
| 18 | 10010 | -2.578 | -0.733 | -3.0 | 3.0 | -6.0 | 0.00 |
| 19 | 10011 | -1.702 | -0.245 | -3.0 | 1.0 | -4.0 | 0.00 |
| 20 | 10100 | -0.968 | 2.499 | -1.0 | 5.0 | -1.0 | 5.196 |
| 21 | 10101 | -1.806 | 1.981 | -3.0 | 5.0 | -2.0 | 3.464 |
| 22 | 10110 | -1.565 | 0.715 | -1.0 | 3.0 | -3.0 | 1.732 |
| 23 | 10111 | -0.50 | 0.50 | -1.0 | 1.0 | -2.0 | 0.00 |
| 24 | 11000 | -1.411 | -2.279 | -5.0 | -3.0 | -4.0 | -3.464 |
| 25 | 11001 | -2.139 | -1.615 | -5.0 | -1.0 | -5.0 | -1.732 |
| 26 | 11010 | -0.485 | -1.65 | -3.0 | -3.0 | -2.0 | -3.464 |
| 27 | 11011 | -1.30 | -1.126 | -3.0 | -1.0 | -3.0 | -1.732 |
| 28 | 11100 | 0.485 | -1.65 | -1.0 | -5.0 | 0.0 | -3.464 |
| 29 | 11101 | -0.492 | -2.634 | -3.0 | -5.0 | -1.0 | -5.196 |
| 30 | 11110 | -0.93 | 1.447 | -1.0 | -3.0 | -1.0 | 1.732 |
| 31 | 11111 | -0.50 | -0.50 | -1.0 | -1.0 | -1.0 | -1.732 |

5

## TABLE 3
## SYMBOL MAPPINGS FOR 64-ary QAM SCHEME

| SYMBOL | BITS | CIRCULAR | | RECTANGULAR | | TRIANGULAR | |
|---|---|---|---|---|---|---|---|
| | | I | Q | I | Q | I | Q |
| 0 | 000000 | 2.758 | 3.286 | 7.0 | 7.0 | 1.0 | 10.0 |
| 1 | 000001 | 3.441 | 2.562 | 7.0 | 5.0 | 8.0 | 0.0 |
| 2 | 000010 | 1.925 | 3.834 | 5.0 | 7.0 | 4.0 | 8.0 |
| 3 | 000011 | 1.867 | 2.399 | 5.0 | 5.0 | 5.0 | 6.0 |
| 4 | 000100 | 0.00 | 4.29 | 1.0 | 7.0 | 0.0 | 8.0 |
| 5 | 000101 | 0.987 | 2.875 | 1.0 | 5.0 | 1.0 | 6.0 |
| 6 | 000110 | 0.989 | 4.174 | 3.0 | 7.0 | 2.0 | 8.0 |
| 7 | 000111 | 0.965 | 1.671 | 3.0 | 5.0 | 3.0 | 6.0 |
| 8 | 001000 | 4.225 | 0.745 | 7.0 | 1.0 | 4.0 | 0.0 |
| 9 | 001001 | 3.939 | 1.699 | 7.0 | 3.0 | 7.0 | 2.0 |
| 10 | 001010 | 2.947 | 0.746 | 5.0 | 1.0 | 5.0 | 2.0 |
| 11 | 001011 | 2.545 | 1.663 | 5.0 | 3.0 | 6.0 | 4.0 |
| 12 | 001100 | 0.866 | 0.50 | 1.0 | 1.0 | 1.0 | 2.0 |
| 13 | 001101 | 0.00 | 1.93 | 1.0 | 3.0 | 2.0 | 4.0 |
| 14 | 001110 | 1.93 | 0.00 | 3.0 | 1.0 | 3.0 | 2.0 |
| 15 | 001111 | 1.671 | 0.965 | 3.0 | 3.0 | 4.0 | 4.0 |
| 16 | 010000 | -3.441 | 2.562 | -7.0 | 7.0 | -1.0 | 10.0 |
| 17 | 010001 | -3.939 | 1.699 | -7.0 | 5.0 | -7.0 | 2.0 |
| 18 | 010010 | -2.758 | 3.286 | -5.0 | 7.0 | -6.0 | 0.0 |
| 19 | 010011 | -1.867 | 2.399 | -5.0 | 5.0 | -5.0 | 6.0 |
| 20 | 010100 | -0.989 | 4.174 | -1.0 | 7.0 | -2.0 | 8.0 |
| 21 | 010101 | 0.00 | 3.04 | -1.0 | 5.0 | -1.0 | 6.0 |
| 22 | 010110 | -1.925 | 3.834 | -3.0 | 7.0 | -4.0 | 8.0 |
| 23 | 010111 | -0.987 | 2.875 | -3.0 | 5.0 | -3.0 | 6.0 |
| 24 | 011000 | -4.225 | 0.745 | -7.0 | 1.0 | -2.0 | 0.0 |
| 25 | 011001 | -2.545 | 1.663 | -7.0 | 3.0 | -6.0 | 4.0 |
| 26 | 011010 | -2.947 | 0.746 | -5.0 | 1.0 | -5.0 | 2.0 |
| 27 | 011011 | -1.671 | 0.965 | -5.0 | 3.0 | -4.0 | 4.0 |
| 28 | 011100 | -0.866 | 0.50 | -1.0 | 1.0 | -1.0 | 2.0 |
| 29 | 011101 | 0.00 | 1.00 | -1.0 | 3.0 | 0.0 | 4.0 |
| 30 | 011110 | -1.93 | 0.00 | -3.0 | 1.0 | -3.0 | 2.0 |
| 31 | 011111 | -0.965 | 1.671 | -3.0 | 3.0 | -2.0 | 4.0 |
| 32 | 100000 | 3.12 | -2.944 | 7.0 | -7.0 | 1.0 | -10.0 |
| 33 | 100001 | 3.715 | -2.145 | 7.0 | -5.0 | 7.0 | -2.0 |
| 34 | 100010 | 2.357 | -3.584 | 5.0 | -7.0 | 6.0 | 0.0 |
| 35 | 100011 | 2.237 | -2.059 | 5.0 | -5.0 | 5.0 | -6.0 |
| 36 | 100100 | 0.498 | -4.261 | 1.0 | -7.0 | 2.0 | -8.0 |
| 37 | 100101 | 0.50 | -2.999 | 1.0 | -5.0 | 1.0 | -6.0 |
| 38 | 100110 | 1.467 | -4.031 | 3.0 | -7.0 | 4.0 | -8.0 |
| 39 | 100111 | 1.447 | -2.674 | 3.0 | -5.0 | 3.0 | -6.0 |
| 40 | 101000 | 4.283 | -0.249 | 7.0 | -1.0 | 2.0 | 0.0 |
| 41 | 101001 | 4.11 | -1.23 | 7.0 | -3.0 | 6.0 | -4.0 |
| 42 | 101010 | 3.03 | -0.251 | 5.0 | -1.0 | 5.0 | -2.0 |
| 43 | 101011 | 2.784 | -1.221 | 5.0 | -3.0 | 4.0 | -4.0 |
| 44 | 101100 | 0.866 | -0.50 | 1.0 | -1.0 | 1.0 | -2.0 |
| 45 | 101101 | 0.00 | -1.93 | 1.0 | -3.0 | 0.0 | -4.0 |
| 46 | 101110 | 1.671 | -0.965 | 3.0 | -1.0 | 3.0 | -2.0 |
| 47 | 101111 | 0.965 | -1.671 | 3.0 | -3.0 | 2.0 | -4.0 |
| 48 | 110000 | -3.12 | -2.944 | -7.0 | -7.0 | -1.0 | -10.0 |
| 49 | 110001 | -3.715 | -2.145 | -7.0 | -5.0 | -8.0 | 0.0 |
| 50 | 110010 | -2.357 | -3.584 | -5.0 | -7.0 | -4.0 | -8.0 |
| 51 | 110011 | -2.237 | -2.059 | -5.0 | -5.0 | -5.0 | -6.0 |
| 52 | 110100 | -0.498 | -4.261 | -1.0 | -7.0 | 0.0 | -8.0 |
| 53 | 110101 | -0.5 | -2.999 | -1.0 | -5.0 | -1.0 | -6.0 |
| 54 | 110110 | -1.467 | -4.031 | -3.0 | -7.0 | -2.0 | -8.0 |
| 55 | 110111 | -1.447 | -2.674 | -3.0 | -5.0 | -3.0 | -6.0 |
| 56 | 111000 | -4.283 | -0.249 | -7.0 | -1.0 | -4.0 | 0.0 |
| 57 | 111001 | -4.11 | -1.23 | -7.0 | -3.0 | -7.0 | -2.0 |
| 58 | 111010 | -3.03 | -0.251 | -5.0 | -1.0 | -5.0 | -2.0 |
| 59 | 111011 | -2.784 | -1.221 | -5.0 | -3.0 | -6.0 | -4.0 |
| 60 | 111100 | -0.866 | -0.50 | -1.0 | -1.0 | -1.0 | -2.0 |
| 61 | 111101 | 0.00 | -1.00 | -1.0 | -3.0 | -2.0 | -4.0 |
| 62 | 111110 | -1.671 | -0.965 | -3.0 | -1.0 | -3.0 | -2.0 |
| 63 | 111111 | -0.965 | -1.671 | -3.0 | -3.0 | -4.0 | -4.0 |

For a random mapping of bits to symbols the probability of bit error is, as $m$ grows large is

$$P_{b\ random} = P_s \frac{2^{m-1}}{2^m - 1}$$

where $m$ is the number of bits per symbol or

$$m = \log_2 M$$

In the case where a symbol error results in only one bit error the conversion is

$$P_{b\ lower} = P_s \frac{1}{m}$$

These results are plotted in Figures 9 - 14 for both *32*-ary and *64*-ary constellations. The solid lines represent the bounds and the marked lines represent the results of a time domain simulation presented in the next section. It should be noted that $P_{b\ lower}$ is not an actual lower bound since it is based on an upper bound the symbol error probability. It is, however, a good indication of the quality of the bit to symbol mappings. In the case of *64-ary* rectangular QAM where the bit to symbol mapping is known to be optimum, the time domain simulation discussed in the next section and the bound agree very well. A modification to the expression for the symbol error probability results in an expression for the bit error probability that takes into account the bit-to-symbol mappings. If $n_{ij}$ is defined as the number of bits that are different in $S_i$ and $S_j$ the upper bound on bit error probability can be written as

$$P_b \leq \frac{2}{M \log_2 M} \sqrt{\frac{1}{2\pi}} \sum_{i=1}^{M-1} \sum_{j=i+1}^{M} n_{ij} \frac{\exp\left(-|S_i - S_j|^2 / 2\sigma^2\right)}{|S_i - S_j| / \sigma}$$

The results of this expression are not plotted to maintain clarity in the figures.

## VI. BIT-ERROR-RATE SIMULATION RESULTS

The BER performance in the AWGN channel is also evaluated by a time domain computer simulation. These simulations are performed to obtain exact measurements of BER that are especially useful at low signal-to-noise ratios where the performance of an error-corrective coded system is very sensitive to "channel" BER. Even though the complete BER curves for the simulation results were presented in this paper, the BER was only simulated at a few $E_b/N_o$ values for both *32-ary* QAM and *64-ary* QAM signal constellations due to the relatively lengthy Monte Carlo BER simulation times.

The simulation models for the *32-ary* QAM and the *64-ary* QAM modems were constructed using the Signal Processing Worksystem™ (SPW) [10]. The simulation models have three main blocks: a modulator; a channel; and a demodulator. Figure 15 is the Euclid Demodulator that is used for all modulations. Figures 16 and 17 show the block diagram for the 32-ary and 64-ary schemes, respectively.
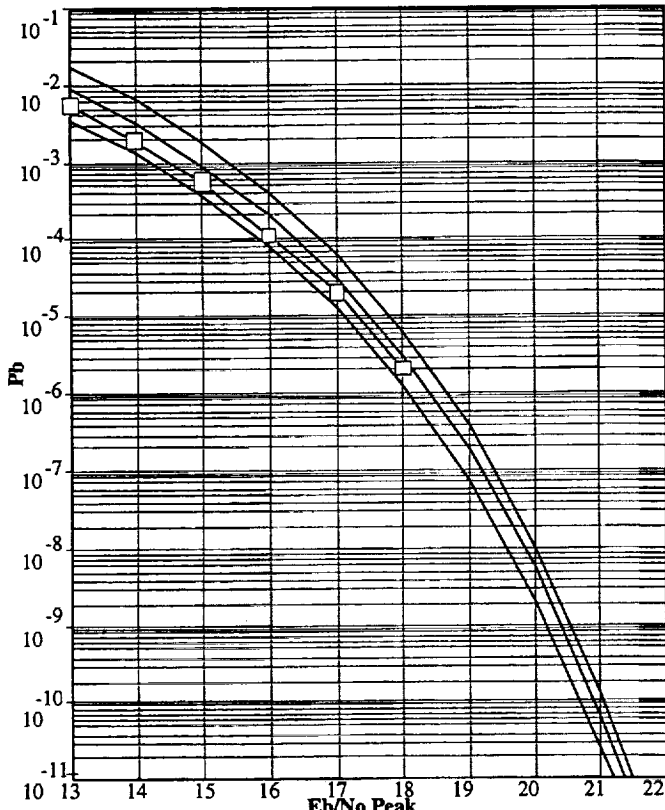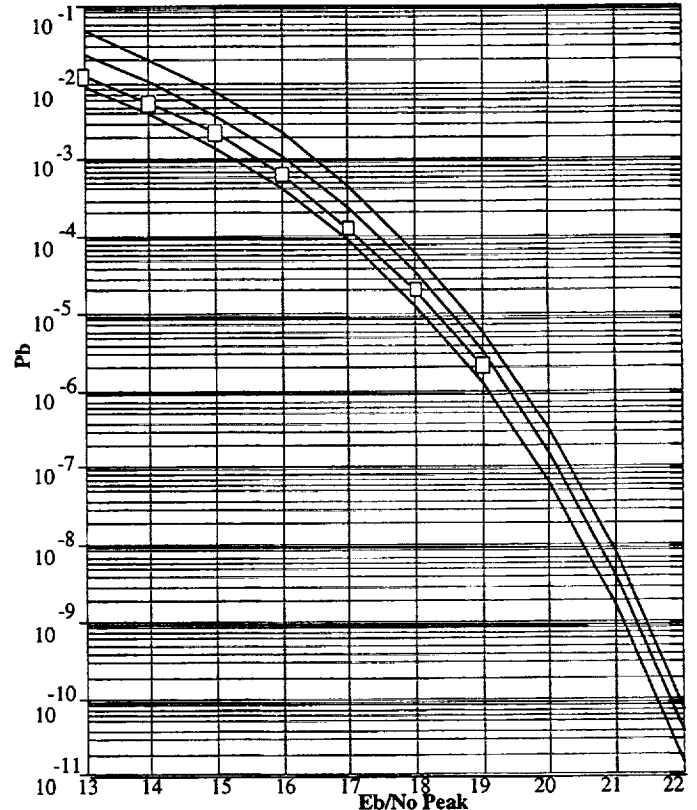
6

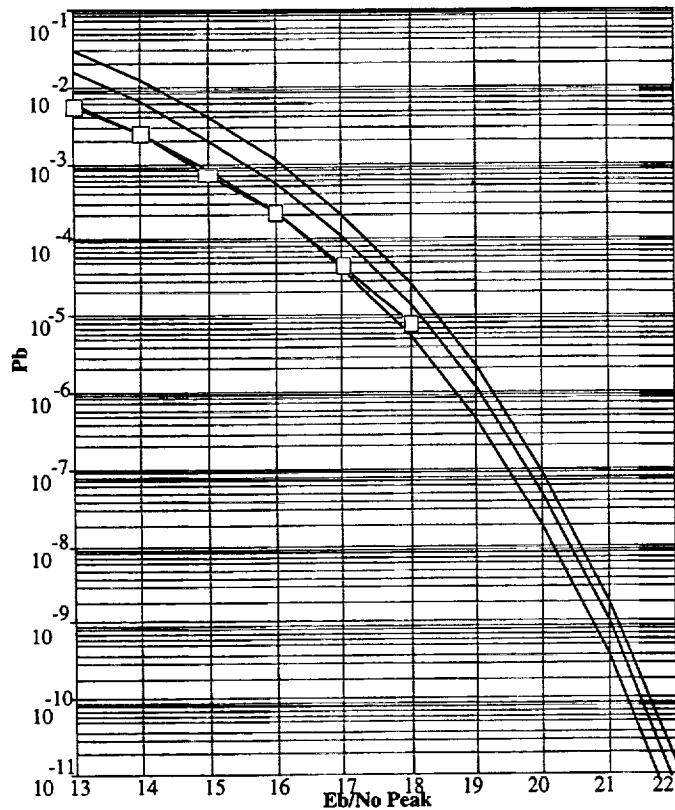FIGURE 9 : 32-ARY CIRCULAR QAM



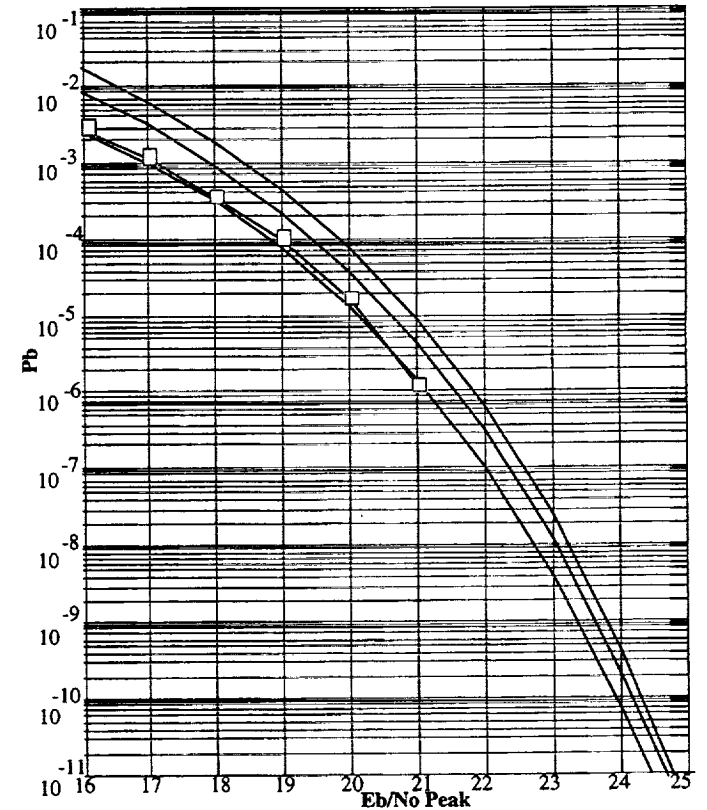FIGURE 11 : 32-ARY TRIANGULAR QAM



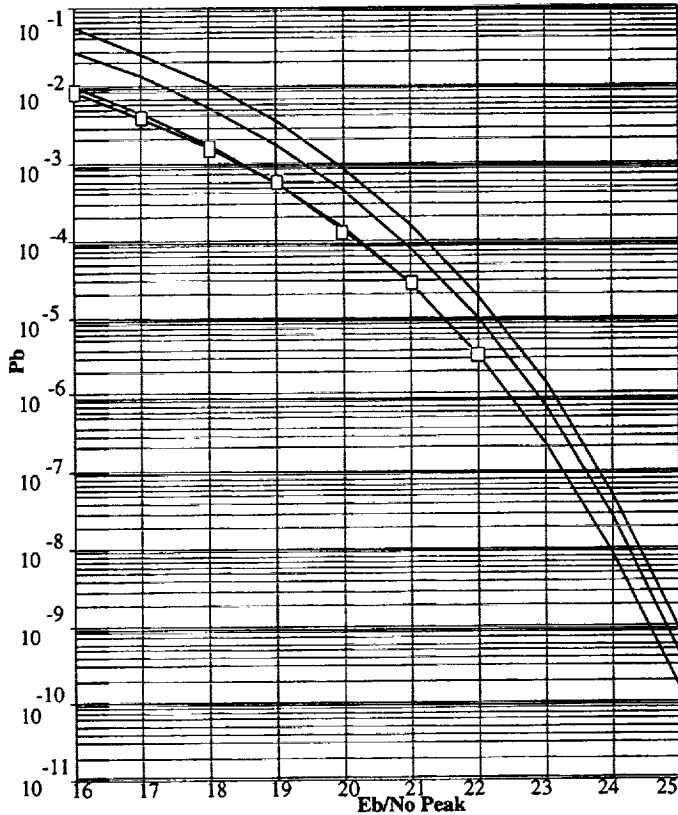FIGURE 10 : 32-ARY RECTANGULAR QAM
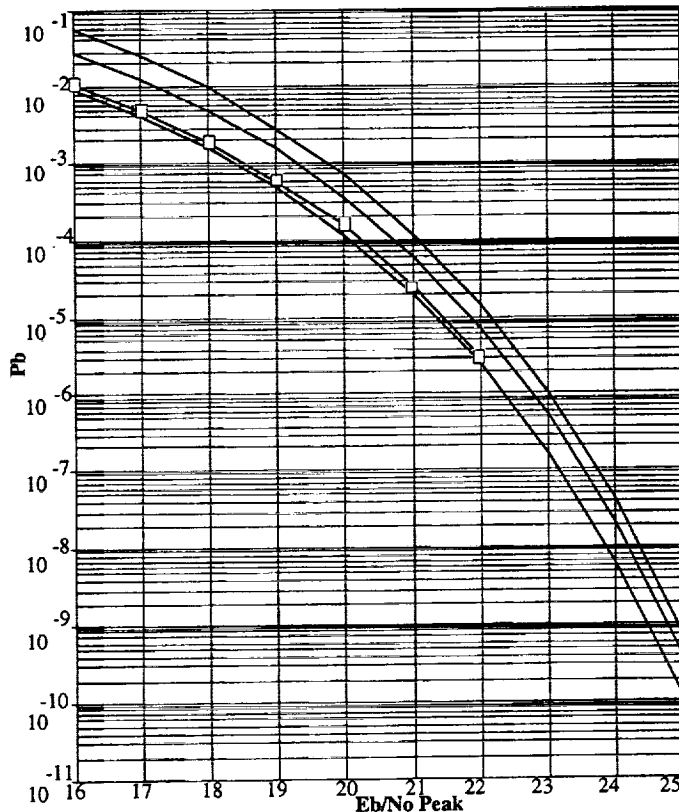


FIGURE 12 : 64-ARY CIRCULAR QAM

7

FIGURE 13 : 64-ARY RECTANGULAR QAM

A modulo $M$ impulse train unit used, as a clock unit, to drive $m$ number of pseudo-random number generators producing binary signal sequences. The $m$ outputs of the pseudo-random generators were multiplied by a factor of two and summed together to form a symbol used to determine the I and Q components of the incoming signal from look-up tables. The look-up tables consist of the in-phase (I) and the quadrature (Q) components corresponding to the real part and imaginary part of all members of a signal set (of either *32-ary* QAM or *64-ary* QAM), respectively as shown in Table 2 and 3. An AWGN source of zero mean and power spectral density $N/2$ is used to add channel noise to the system in order to vary the SNR. The generated sequence of AWGN generator is added to the main signal. At the demodulator, the transmitted symbol is determined by calculating the Euclidian distances between the received signal and all members of the signal set and by selecting the one has a minimum Euclidian distance. The resulting symbol at the demodulator then passes through a symbol-to-bit converter unit. The BER of the system is then calculated by comparing each bit of the resulting symbol to corresponding bit of the original symbol.

**TABLE 4**

Peak and Average Eb/No at Pb=1.0E-6

| Signal Constellation | Unfiltered Peak Eb/No | Filtered Peak Eb/No | Unfiltered Avg. Eb/No |
|---|---|---|---|
| 32-ary (4, 11, 17) Circular QAM | 18.30 dB | 20.37 dB | 16.63 dB |
| 32-ary Rectangular QAM | 18.80 dB | 20.87 dB | 16.50 dB |
| 32-ary Triangular QAM | 19.25 dB | 21.32 dB | 16.42 dB |
| 64-ary (6, 12, 19, 27) Circular QAM | 21.10 dB | 23.17 dB | 18.98 dB |
| 64-ary Rectangular QAM | 22.45 dB | 24.52 dB | 18.77 dB |
| 64-ary Triangular QAM | 22.35 dB | 24.42 dB | 18.69 dB |

The performance of both *32-ary* QAM and *64-ary* QAM signal constellations has been evaluated by the analytical expression of the symbol error probability as discussed in Section V. The BER plots of the simulation results of both signal constellations are shown in Figures 9 - 14. For *32-ary* QAM signal constellations, the (4, 11, 17) circular is superior by about *0.95 dB* to the triangular constellation and by about *0.50 dB* to the rectangular constellations on the basis of Unfiltered Peak SNR. For *64-ary* QAM signal constellations, the (6, 12, 19, 27) circular constellation yields the best unfiltered peak SNR performance but the triangular and rectangular constellations are only inferior by *1.25 dB* and *1.35 dB*,



FIGURE 14 : 64-ARY TRIANGULAR QAM

8

Euclid 2-D Demodulator
Parameters

inphase_filename...    'kifsigs/I32triqam'
quadrature_filename...'kifsigs/Q32triqam'
# of constellation points...32

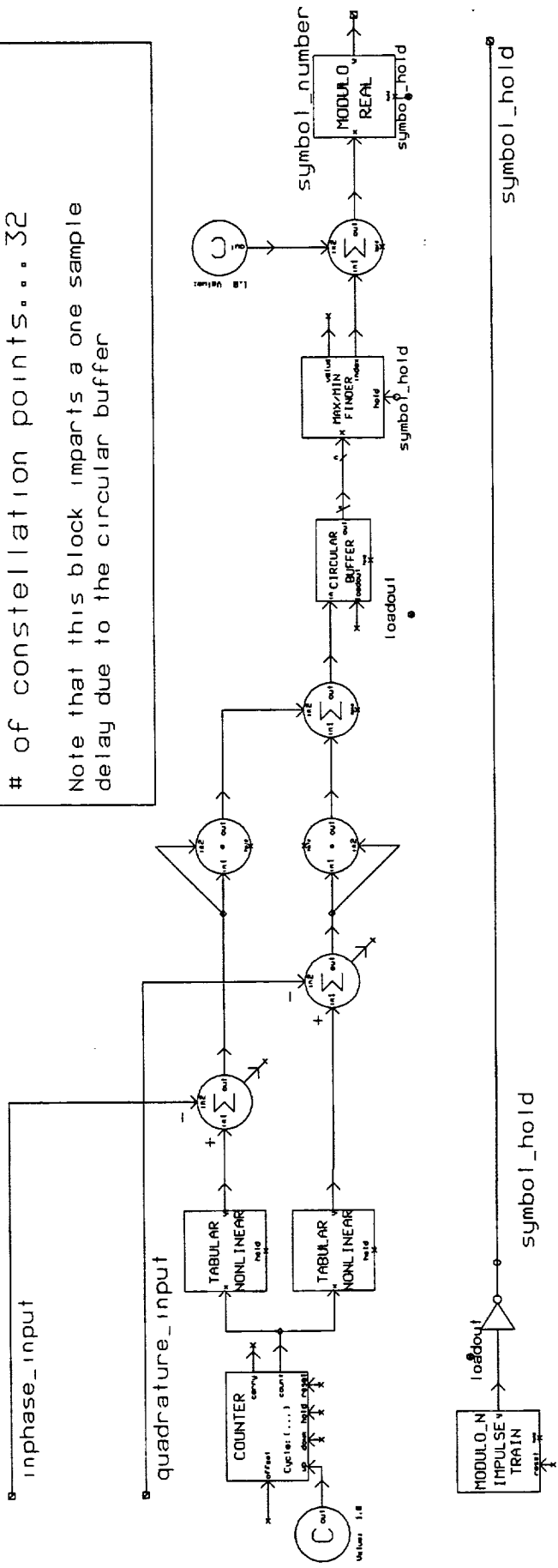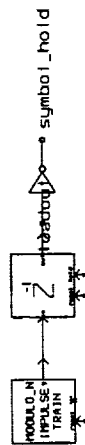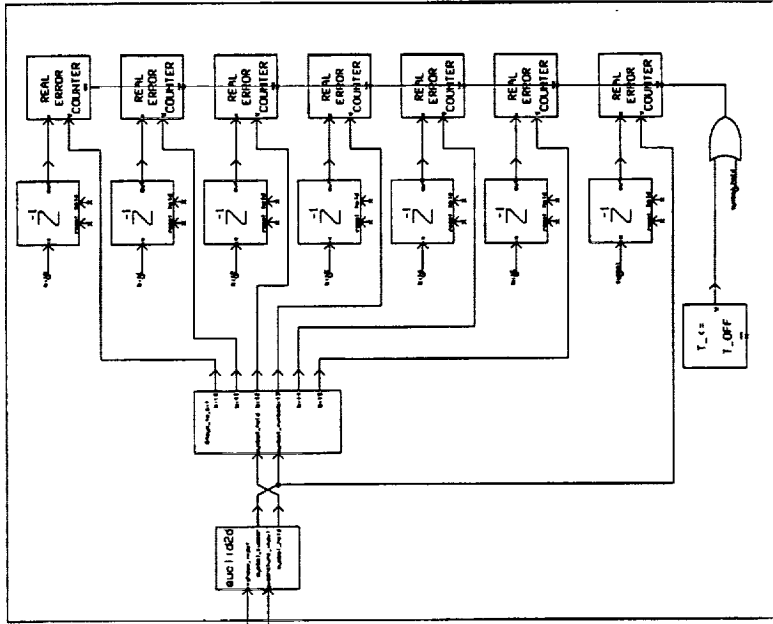Note that this block imparts a one sample
delay due to the circular buffer

inphase_input

quadrature_input

symbol_hold

symbol_number

symbol_hold

symbol_hold

**Figure 15.—Euclid Demodulator.**

9

symbol rate....           1.0

sample frequency...       1.0

Es/No...                  23.8

Print Estimate Modula...1000

64-ary (6,12,19,27) Circular QAM Demodulator
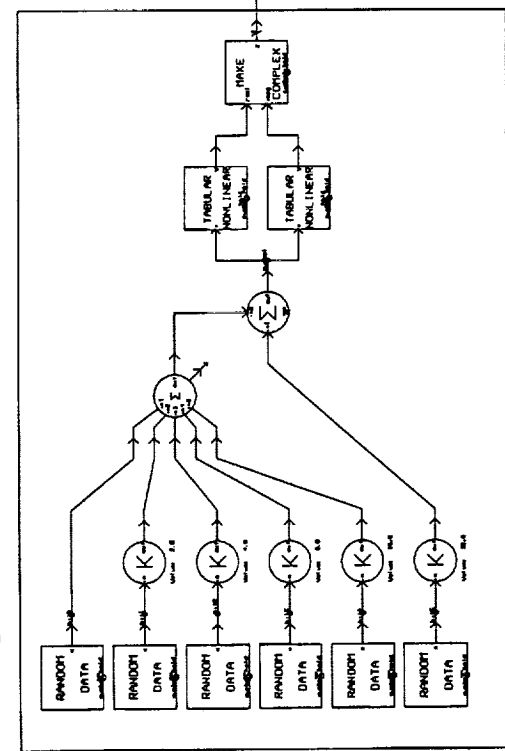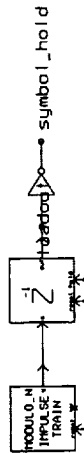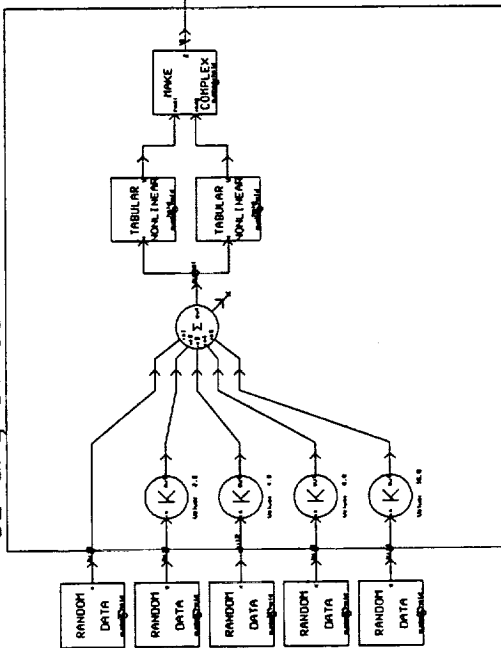
64-ary (6,12,19,27) Circular QAM Modulator

symbol_hold

MODULO_N IMPULSE TRAIN

REAL ERROR COUNTER

COMPLEX TO REAL/IMAG

euclidean

T_OFF

COMPLEX WHITE NOISE

RANDOM DATA

MAKE COMPLEX

TABULAR NONLINEAR

**Figure 16.—64-QAM System.**

10

32-ary Circular QAM Demodulator

REAL ERROR COUNTER (×6)

$Z^{-1}$ (×6)

32ary_hold

Euclid2d

COMPLEX TO REAL/IMAG

T_<=
1_OFF

symbol rate....      1.0
sample frequency...  1.0
Es/No...            20.0
Print Estimate Modula...5000

$Z^{-1}$

random

symbol_hold

MODULO_N IMPULSE TRAIN

32-ary Circular QAM Modulator

MAKE COMPLEX

TABULAR NONLINEAR

TABULAR NONLINEAR

COMPLEX WHITE NOISE

·K·

·Σ·

·K·

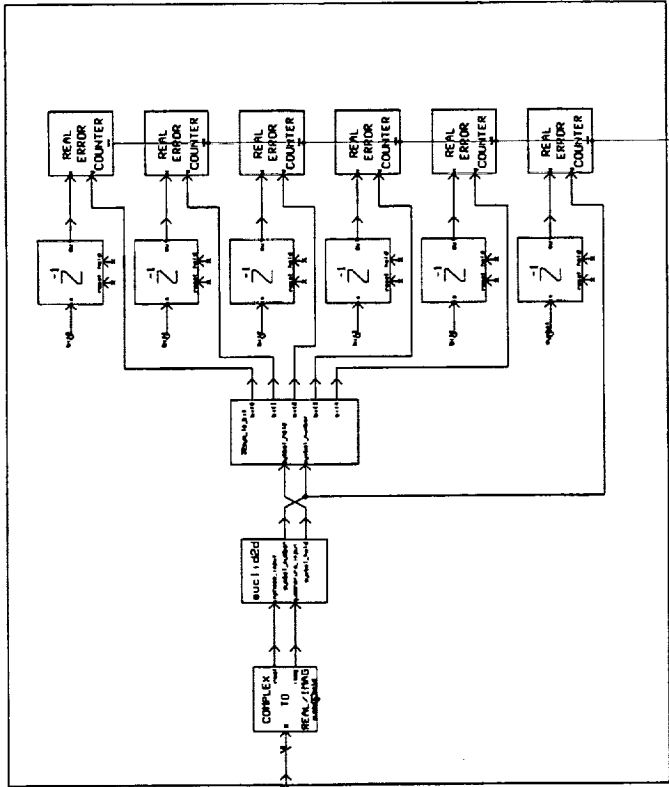RANDOM DATA (×5)

·K·  ·K·  ·K·  ·K·
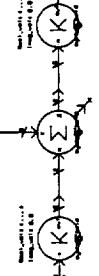
Figure 17.—32-QAM System.

respectively. The simulation results of both signal constellations are summarized in Table 4 for peak and average $E_b/N_o$ at BER of 1.0E-6. The circular constellations thus provide the best peak SNR performance over both triangular and rectangular signal constellations as indicated in Table 4.

## VII. CONCLUSIONS

The BER performance of both *32-ary* QAM and *64-ary* QAM signal constellations over the AWGN channel has been presented. As summarized in Table 4, the circular constellations provide the best peak SNR performance over both triangular and rectangular signal constellations since the circular constellations populate as many symbols as possible at the peak magnitude. The circular QAM modulation schemes are thus regarded as the best techniques for bandwidth efficiency, and the increased power requirements to implement the schemes may be absorbed through the use of advanced High Power Amplifiers (HPA) such as Microwave Power Modules (MPM). It is also shown that the effect of shaping the baseband data results in about a *2 dB* loss in signal power due to backing off the HPA to account for filtered signal excursions.

Topics for future study include the significant benefit of combined modulation and coding techniques that can further ease the power requirements over uncoded schemes. Further, coding may be a good technique to control the peak filtered power excursions. Also, the results presented in this paper provide good basics for a continuation effort in the development of a combined modem and codec hardware that can accommodate B-ISDN at rate of *155.52 Mbps* through typical transponder bandwidths of *36 MHz* and *54 MHz*.

## VIII. REFERENCES

[1]    D.H. Martin, "Communication Satellites 1958-1992," Published by The Aerospace Corporation, Dec. 1991.

[2]    F. Hemmati, S. Miller, "A B-ISDN Compatible Modem/Codec," *Proceedings of the NASA Space Communications Technology Conference*, NASA CP-3132, pp. 247-253, Nov., 1991.

[3]    J. Tague, L. Shimoda, "High Precision Waveform Precompensation for Optimal Digital Signaling," Final Report to NASA LeRC, June 1992.

[4]    G. Karam, H. Sari, "A Data Predistortion Technique with Memory for QAM Radio Systems," *IEEE Trans. Commun.*, vol. 39, No. 2 , pp. 366-344, Feb., 1991.

[5]    G. Feng, et al, "A Modified Adaptive Compensation Scheme for Nonlinear Bandlimited Satellite Channels," Globecom '91, pp. 1551-1555, Dec. 1991.

[6]    K. Konstantinides, K. Yao, "Modelling and Computationally Efficient Time Domain Linear Equalisation of Nonlinear Bandlimited QPSK Satellite Channel," *IEE Proc.*, vol. 137, pt. I, no. 6, pp. 438-442, Dec. 1990.

[7]    S.W. Chueng, "Influence of Signal Constellation on the Performance of 16-ary DEQAM Transmission Through a Regenerative Satellite Link," *Int. Jou. of Satellite. Commun.*, vol. 8, pp. 65-77, 1990.

[8]    E. Bilgieri, et al, "Analysis and Compensation of Nonlinearities in Digital Transmission Systems, " *IEEE Jou. Sel. Commun.*, vol. 6, no. 1, pp. 42-51, Jan. 1989.

[9]    C.M. Thomas, et al, "Digital Amplitude-Phase Keying with M-ary Alphabets," *IEEE Trans. Commun.*, vol. COM-22, pp. 168-180, Feb., 1974.

[10]   SPW$^{TM}$ - The DSP Framework$^{TM}$, User's Guide and Tutorial, Comdisco Systems, Inc, 1992.

# REPORT DOCUMENTATION PAGE

Public reporting burden for this collection of information is estimated to average 1 hour per response, including the time for reviewing instructions, searching existing data sources, gathering and maintaining the data needed, and completing and reviewing the collection of information. Send comments regarding this burden estimate or any other aspect of this collection of information, including suggestions for reducing this burden, to Washington Headquarters Services, Directorate for Information Operations and Reports, 1215 Jefferson Davis Highway, Suite 1204, Arlington, VA 22202-4302, and to the Office of Management and Budget, Paperwork Reduction Project (0704-0188), Washington, DC 20503.

| 1. AGENCY USE ONLY (Leave blank) | 2. REPORT DATE | 3. REPORT TYPE AND DATES COVERED |
|---|---|---|
| | February 1994 | Technical Memorandum |

**4. TITLE AND SUBTITLE**

Bounds and Simulation Results of 32-ary and 64-ary Quadrature Amplitude Modulation for Broadband-ISDN via Satellite

**6. AUTHOR(S)**

Muli Kifle and Mark Vanderaar

**5. FUNDING NUMBERS**

WU–235–01–04

**7. PERFORMING ORGANIZATION NAME(S) AND ADDRESS(ES)**

National Aeronautics and Space Administration
Lewis Research Center
Cleveland, Ohio 44135–3191

**8. PERFORMING ORGANIZATION REPORT NUMBER**

E–8470

**9. SPONSORING/MONITORING AGENCY NAME(S) AND ADDRESS(ES)**

National Aeronautics and Space Administration
Washington, D.C. 20546–0001

**10. SPONSORING/MONITORING AGENCY REPORT NUMBER**

NASA TM–106484

**11. SUPPLEMENTARY NOTES**

**12a. DISTRIBUTION/AVAILABILITY STATEMENT**

Unclassified - Unlimited
Subject Category 17

**12b. DISTRIBUTION CODE**

**13. ABSTRACT (Maximum 200 words)**

Union bounds and Monte Carlo simulation Bit-Error-Rate (BER) performance results are presented for various *32-ary* and *64-ary* Quadrature Amplitude Modulation (QAM) schemes. Filtered and unfiltered modulation formats are compared for the best packing arrangement in peak power limited systems. It is verified that circular constellations which populate as many symbols as possible at the peak magnitude offer the best performance. For example: a *32-ary* QAM scheme based on concentric circles offers about *1.05 dB* better peak power improvement at a BER of $10^{-6}$ over the scheme optimized for average power using triangular symbol packing. This peak power improvement increases to *1.25 dB* for comparable *64-ary* QAM schemes. This work serves as a precursor to determine the feasibility of a combined modem/codec that can accommodate Broadband Integrated Services Digital Network (B-ISDN) at a rate of *155.52 Mbps* through typical transponder bandwidths of *36 MHz* and *54 MHz*.

**14. SUBJECT TERMS**

M-ary Quandrature Amplitude Modulation; Broadband-ISDN; High Power Amplifiers; Satellite Communications

**15. NUMBER OF PAGES**

13

**16. PRICE CODE**

A03

| 17. SECURITY CLASSIFICATION OF REPORT | 18. SECURITY CLASSIFICATION OF THIS PAGE | 19. SECURITY CLASSIFICATION OF ABSTRACT | 20. LIMITATION OF ABSTRACT |
|---|---|---|---|
| Unclassified | Unclassified | Unclassified | |